Biomedical Physics &
Engineering Express

Endorsed by IPEM Institute of Physics and Engineering in Medicine
PURPOSE-LED PUBLISHING™

PAPER • **OPEN ACCESS**

An investigation of a passive BCI's performance for different body postures and presentation modalities

To cite this article: Diana E Gherman *et al* 2025 *Biomed. Phys. Eng. Express* **11** 025052

Biomedical Physics & Engineering Express

PAPER

An investigation of a passive BCI's performance for different body postures and presentation modalities

Diana E Gherman[1,2], **Laurens R Krol**[2], **Marius Klug**[2,3] and **Thorsten O Zander**[1,2]

[1] Chair of Neuroadaptive Human-Computer Interaction, Brandenburg University of Technology Cottbus-Senftenberg, Cottbus, Germany
[2] Zander Laboratories GmbH, Cottbus, Germany
[3] Young Investigator Group—Intuitive XR, Brandenburg University of Technology Cottbus-Senftenberg, Cottbus, Germany

E-mail: diana.gherman@b-tu.de

Keywords: passive brain-computer interfaces, virtual reality, workload, posture, EEG, passive BCI, pBCI

OPEN ACCESS

RECEIVED
12 June 2024

REVISED
6 February 2025

ACCEPTED FOR PUBLICATION
13 February 2025

PUBLISHED
27 March 2025

Abstract

Passive brain-computer interfaces (passive BCIs, pBCIs) enable computers to unobtrusively decipher aspects of a user's mental state in real time from recordings of brain activity, e.g. electroencephalography (EEG). When used during human-computer interaction (HCI), this allows a computer to dynamically adapt for enhancing the subjective user experience. For transitioning from controlled laboratory environments to practical applications, understanding BCI performance in real contexts is of utmost importance. Here, Virtual Reality (VR) can play a unique role: both as a fully controllable simulation of a realistic environment and as an independent, increasingly popular real application. Given the potential of VR as a dynamic and controllable environment, and the capability of pBCIs to enable novel modes of interaction, it is tempting to envision a future where pBCI and VR are seamlessly integrated. However, the simultaneous use of these two technologies—both of which are head-mounted—presents new challenges. Due to their immediate proximity, electromagnetic artifacts can arise, contaminating the EEG. Furthermore, the active movements promoted by VR can induce mechanical and muscular artifacts in the EEG. The varying body postures and display preferences of users further complicate the practical application of pBCIs. To address these challenges, the current study investigates the influence of body posture (sitting Versus standing) and display media (computer screen Versus VR) on the performance of a pBCI in assessing cognitive load. Our results show that these conditions indeed led to some changes in the EEG data; nevertheless, the ability of pBCIs to detect cognitive load remained largely unaffected. However, when a classifier trained in one context (body posture or modality) was applied to another (e.g., cross-task application), reductions in classification accuracy were observed. As HCI moves towards increasingly adaptive and more interactive designs, these findings support the expansive potential of pBCIs in VR contexts.

1. Introduction

1.1. Current and future uses of passive brain-computer interfaces (pBCIs)

Since their initial definition [1, 2], passive brain-computer interfaces (passive BCI, pBCI) have demonstrated the capability of decoding different cognitive states in real time from brain activity. As such, they can provide real-time information to a computer about its user's cognitive states, including surprise [3] workload [4, 5] or error-perception [6], as well as affective states [7]. This creates an implicit human-computer communication channel and enables technology to become neuroadaptive [8]. This technological ability to decode and adapt to human mental states, unobtrusively and in real time, can translate into a wide range of use cases across fields like education [9], driving [10, 11], aviation [12, 13], neuromarketing [14], gaming [15] and more.

In the context of an increasingly digitized world and the rise of the Internet of Things, this diversity of use cases and versatility make the pBCI technology attractive for future adoption. As society transitions into a more cyber-connected age, the need for more intuitive modalities of interaction with machines that

lead to a more immersive communication will increase [16]. What makes pBCI a good candidate to fulfill this role is its reliance on natural streams of brain activity, that require no effort on the human part [2]. A recent surge in BCI research innovations [17] and commercial interest [18] in neuroscience in general and pBCI in particular [19] is indicative of the current momentum aiming at widespread adoption of BCI.

This perspective is supported by several examples of pBCI that are aimed at real-world use [20]. Nevertheless, the transition to applications in our daily lives is still ongoing and several hurdles need to be overcome. The reason for this is multi-fold. EEG devices are still impractical [18], they tend to be unreliable in uncontrolled environments [21], and they require time-consuming calibration phases [22]. Specifically, the calibration phases are necessary because classifiers have been shown to be sensitive to the task [23], subject [24], sensors [25], and even the context in which they are being applied [26]. Therefore, it is important to investigate if pBCIs remain performant across various situations, without the need to re-train classifiers. In light of this, we here assess to what extent pBCI performance is influenced by different contexts, particularly different postures and virtual environments. We refer to this as cross-context performance.

1.2. The impact of body posture on brain activity and pBCI performance

Most human activities, especially at the workplace, involve intermediary positions, like daily office work, where we constantly switch between sitting, standing, and various postures. Even in more specialized workplaces, such as surgery, doctors might stand for prolonged periods but switch to sitting every so often. Similarly, working at a desk with a computer, a person might stretch, adjust their position, or lean back. This constant movement is an essential characteristic of human bodies and it helps us to better interact with and learn from the environment. Thus, this fact needs to be taken into consideration when assessing the integration of BCI into our daily lives by looking at the effective use of the technology across body positions. While both sitting and standing are common postures, standing has been less examined in BCI research despite studies that found potential variations in neural signals [27–29].

For instance, in the field of Mobile Brain/Body Imaging (MoBI) [30, 31], differences in brain activity between sitting and standing have been observed. Also, an fMRI investigation found that, in comparison with a supine position, the upright posture increases the high-frequency oscillatory activity [27].

Concerning EEG, it is currently unclear how body posture affects the signal. Some studies suggest that there are no significant differences in spectral variations between the sitting and the standing positions for rest alpha (8–12 Hz) [28]. Meanwhile, [32] did find differences at the level of the alpha band, albeit for patients suffering from a balance disorder. Other findings indicate an increase in power for fast oscillatory bands such as beta and gamma if participants stand up [33, 34]. Interesting insights come from complexity analyses in recent studies, which show that standing induces smaller values of brain activation compared to walking [29]. Complexity variations across postural conditions have proven valuable for entropy-based BCIs [35]. A potential explanation for such differences comes from [36]. The authors argue that changing positions might result in a physical shift of the brain, and the associated small changes in cerebrospinal fluid could affect the electrical fields, a claim that has also been tested and confirmed by [37]. Alternatively, researchers speculate the underlying causes could be related to the fact that an upright position determines the aggregate activity of the trunk and muscle activity variations [38]. This could lead to more muscle artifacts being mixed with the cortical activity, which might also pose an obstacle to the detection and classification of mental states (*muscle argument*). In the context of BCI, differences have been observed between sitting and standing postures, but only in the context of active motor imagery [39, 40] or P300-based BCI [41]. The need for this work is especially pressing in light of research [38] and new technologies such as VR that require pBCI users to stand.

Additionally, recent health findings and recommendations emphasize the need to decrease sitting time. While most high-income jobs are performed at desks [42], a significant increase in mortality can be observed among those who sit for long hours daily [43], irrespective of other factors such as smoking or regular exercise [44]. As clinical conclusions start to accumulate and public health communication begins to take effect, we can see a rise in standing desk purchases [45], both in the educational sector [46] and the corporate sector [47]. Studies that contrasted the cognitive performance in different body postures support the benefits of this growing trend, suggesting that brain efficiency is higher during standing and sitting compared to a supine position [48] and an increase in attention can be observed when standing compared to sitting, in tasks that simulate attending lectures [49] or performing psychomotor vigilance tasks [50].

Considering all the aforementioned factors, we take a first step here towards comparing the robustness of pBCI during sitting and standing. The standing posture serves as a notable instance of various potential body positions that may become pertinent for practical applications of this technology. To the best of our knowledge, there are no existing studies that have investigated the impact of body postures on pBCI performance.

1.3. Virtual reality's prospective impact on pBCI

Virtual reality (VR) represents one of the biggest present-day shifts in the realm of HCI, specifically

moving users from seated to more mobile positions, as espoused by start-ups and commercial giants alike [51]. It remains to be seen if VR will become the promised default we turn to for social media, remote work, and games, but the general abundance of VR devices and increased number of users, as well as the growing interest and investment in this technology in industries such as healthcare [52] and education [53] speak in favour of, at the very least, widespread adoption of the technology. With VR and pBCI both gaining ground, we must assess their compatibility with each other. The questions posed here are exactly those that need to be answered for this assessment: How is a pBCI classifier affected by the presence of the VR device itself, and how is it affected by the different postures (sitting and standing) primarily afforded by VR?

So far, the scientific literature merging BCI and VR generally explored how decoded brain activity can be utilized to manipulate virtual objects or navigate in virtual environments [54–56]. As such, these papers mostly focus on active BCI, while there are much fewer examples of merging pBCI and VR [57–59]. For instance, some studies involved passively monitoring cognitive workload in virtual environments [60, 61], while others used such information to adapt the difficulty or other characteristics of a task [62, 63] and promote engagement [64]. This line of research lays the foundation for neuroadaptive work training or educational applications in VR, promising truly personalized learning settings [65]. Similarly, pBCI-VR studies created customized therapeutic experiences by adapting virtual stimuli to real-time translated emotional user states [66–68]. Specifically, VR proves to be a beneficial tool in exposure therapy for mental disorders like height phobia (acrophobia) or social anxiety, as it offers the possibility to easily and automatically modulate such phobic stimuli (e.g. the number of avatars in an audience in the context of a public speech) to foster the targeted psychological changes according to psychiatric individual needs [69]. This feature is not necessarily as readily available or easy in ecological conditions. Such qualities render VR an indispensable resource for studying human-machine interaction and a perfect complement to pBCIs both for cognitive and affective state elicitation and neuroadaptive purposes [65].

An interesting example of a potential way pBCIs might be used by real VR consumers is a recent application of a 'concentration' decoder in a popular VR game called Skyrim VR . In this modification, players' brain activity is sensed via a *Muse* commercial EEG headband [70]. Depending on the achieved cognitive focus level, the game character can 'recharge' its powers and better fight virtual enemies. We speculate that such games will most probably be played in a dynamic fashion while standing.

It is unclear if the pBCIs' capability in cognitive state decoding is impacted by mounting a second piece of equipment over an EEG cap. The worries stem from EEG sensors' susceptibility to pressure variations and external artifacts, which might in turn impact the signal the classifier is based on. Prior research investigated and partly confirmed this *signal-to-noise ratio (SNR) argument* [71, 72].

In addition to issues of user comfort [73, 74], the alternations in EEG signal quality when mounting an HMD VR device on top of an EEG cap were studied by [71] using an oddball paradigm in 3 display modalities: HMD-VR, cave automatic VR (CAVE VR), and computer screen. Their analyses revealed that although the HMD-VR and EEG combination is feasible and event-related potentials were valid for all conditions, a custom modification of the HMD strap might be needed to improve the SNR. Another study discovered the signal was unaffected in frequencies under 50Hz, but over this threshold, HMDs do introduce large artifacts [72].

These findings are valuable insights for the VR-EEG research and applications, but the impact of HMD-VR on pBCIs' decoding function has yet to be investigated. While the general impact of VR usage on pBCI requires more research, the role of user posture in VR-EEG research also needs a closer look. Notably, standing is a highly used posture in VR experiences [75], adding another layer of complexity to the interaction between these two technologies. Nonetheless, most VR-EEG studies still involve performing immersive tasks while sitting.

1.4. Investigating pBCI performance across different conditions

In the previous paragraphs, we emphasized the importance of assessing the pBCI capabilities in more realistic conditions. In the study presented here, we are taking steps towards this goal. It is, of course, not feasible to anticipate and evaluate across all potential settings. Therefore, our work focused on two important dimensions: body posture and presentation modality. More specifically, a within-subject design was used to compare the performance of a mental workload classifier between sitting versus standing body posture, and VR versus computer screen presentation modality, as well as the differences in signal across the four possible conditions. We chose to investigate a workload paradigm because there are clear, validated signals associated with high Versus low levels of cognitive workload [23, 76, 77]. Here, an increase in frontal theta and a decrease in parietal alpha should be expected when a high mental workload is experienced, while viceversa is anticipated for a low level of workload. Therefore, we specifically chose to look at the alpha and theta band changes during rest time to identify the signals indicating low workload. Both alpha and theta bands during rest or internally directed attention states have been previously associated with the brain's default mode network (DMN) [78, 79]. We assume that adding a head-mounted

device or standing up would increase the cognitive effort required for the task, causing a switch to an extrinsic mode network (EMN) [79] and resulting in alpha and theta bands changes. Furthermore, shifts of these alpha and theta baselines might affect the calibration outcomes [80] for a brain-computer interface, potentially resulting in decreased classification performance. We also addressed cross-context application capabilities by looking at the generalizability of the workload classifier in the different contexts of body postures and task presentation modalities. Our research questions and hypotheses were the following:

RQ1: Does the modality of task presentation or posture affect the power in the rest alpha and rest theta frequency bands, the signal-to-noise ratio and muscle activity?

H1.1. Variations in the modality of task presentation will have a significant impact:

H1.1.1. on the parietal rest alpha and frontal rest theta activity

H1.1.2. on the signal-to-noise ratio

H1.2. Variations in posture will have a significant impact:

H1.2.1. on the muscle signal

H1.2.2. on the parietal rest alpha and frontal rest theta activity

H1.2.3. on the signal-to-noise ratio

More specifically, we expected significant differences in the power of frontal rest theta and parietal rest alpha frequencies between VR and computer screen modalities, as well as sitting and standing postures. Additionally, we predicted differences in the signal-to-noise ratios based on both task presentation modality and posture. We expected to see stronger muscle signal in the standing posture condition.

RQ2: Does the modality of task presentation or posture matter for the pBCI's ability to decode mental states?

We postulated that the decoding accuracy would significantly vary depending on the context due to potential alterations in the EEG signal patterns due to changes associated with muscle activity during standing or with the addition of VR devices.

H2.1. The modality of task presentation during task execution will significantly affect the pBCI's ability to decode mental states.

H2.2. The body posture during task execution will significantly affect the pBCI's ability to decode mental states.

RQ3: How well can classifiers generalize across body posture and stimulus presentation modality conditions?

H3: Changes between conditions in body posture and presentation modality significantly impact the cross-context application performance of a pBCI. It is hypothesized that classifiers trained in one context (e.g., sitting while viewing a computer screen) may show reduced performance when tested in a different context (e.g., standing while using VR), due to the different cognitive and physical conditions associated with these contexts.

2. Methods

2.1. Participants

A pilot phase involving 3 participants was conducted before the official study began. This helped us find suitable adjustments to maximize participants' comfort in the VR conditions. Afterward, 24 participants were recruited. Two participants were excluded from the final analyses because impedances on the electrodes could not be reduced to an acceptable level (under 20 kΩ) or technical software issues during the recording. The final sample had an equal representation of sexes, consisting of 11 males and 11 females, with a mean age of 27.70 years (SD = 4.78). Participants gave informed consent before the start of the session. Ethics approval was obtained through the institution's ethics committee.

2.2. Apparatus and materials

2.2.1. Computer screen and VR conditions setup

In the computer screen (CS) modality condition, participants sat (*CS-sit*) or stood upright (*CS-stand*) in front of a 61 cm LCD monitor about one meter away with the top of the monitor approximately aligned with the top of the participant's head. In the standing condition, a monitor stand was placed under the monitor to adjust for the height.

For the VR modality (VR) condition, an HP Reverb G2 Omnicept [81] HMD-VR Headset was applied over the EEG cap. Before every VR condition (*VR-sit* and *VR-stand*), an eye calibration was performed with the headset's internal software, which also helped ensure the same headset positioning across participants. To familiarise themselves with the VR environment, the participants were given 3–5 min before the first VR condition to look around the virtual space. We used the NightSkyPlatform in Windows Mixed Reality feature to project a virtual computer screen as in the CS modality condition, as seen in figure 1. The virtual screen was placed in a standard way, at the edge of a circular standing platform.

Participants were instructed to position themselves exactly in front of the virtual screen and in the middle of the platform before starting the task. The same experimental task was presented on the real and virtual computer screen in the CS and VR conditions, respectively.

2.2.2. The workload-inducing task

The task, which was presented 4 times for each participant (once per condition), was a previously tested paradigm [23, 82] called the 'sparkles paradigm'. Simulation and Neuroscience Application Platform (SNAP) [83] was used to present the stimuli. The task

Figure 1. Task display in the VR conditions.

consisted of 40 10-second trials of alternating high workload and no workload trials (20 high, 20 with no workload). These trials were presented in two blocks, with a self-paced break in between (20 total trials for each block, each resulting in 200 seconds of EEG). During the high workload conditions, participants were presented with an equation of the form 'A—B' on a black background. A could be a number between 200 and 1200 and B ranged from 6 to 19, not including 10 and 15. The participants' task was to continuously subtract B from A until the equation disappeared from the screen. For example, if the equation appearing on the real or virtual screen was 1103–*7*, participants had to mentally calculate 1096, 1089, 1082. To make sure the participants understood the task, we gave a trial run with instructions at the beginning.

In the no workload condition, a crosshair was presented in the middle of the screen. For this part, we instructed participants to relax with open eyes by either trying to think of nothing and focus on their breathing or choosing in advance a relaxing memory to bring back into mind.

In half of the trials, under both high and no workload conditions, 10 small 'sparkles' moved smoothly across the screen following random paths created by Perlin noise. This served as a visual distraction and assisted in balancing eye movements evenly across different classes.

To ensure engagement, participants had to type in the number they arrived at for 25% of the trials if in CS modality or verbally communicate the number if in VR modality, which was then typed into the system by the experimenter. The mean accuracy of their responses was 68%, with a variance of 8.

2.2.3. EEG recording

For EEG recording, 64 active actiCAP slim gel electrodes (Brain Products GmbH, Gilching, Germany) were used according to the 10–20 international system [84] and the signal was sampled at 500 Hz using an actiCHamp amplifier. The electrodes were referenced to FCz and the ground electrode was set on the TP9 electrode. We chose this configuration to deal with the potential friction with the VR device in the frontal region. All electrode impedances were kept under 20 kΩ. The VR device's incorporated sensors allowed the recording of heart rate, eye-tracking, and a measure of cognitive load. While these measures were recorded at the same time as the EEG signal, they will be used for subsequent analyses not present in this paper to explore other research questions. The Lab Streaming Layer (LSL) [85] was used to synchronize the channel streams.

2.2.4. Questionnaires

To account for the potential confounding effects of susceptibility to VR sickness, participants completed the short version of The Motion Sickness Susceptibility Questionnaire (MSSQ) [86]. The responses were inspected by the experimenter on the spot, but they were not included in the data analysis. Also, after each VR condition, the Virtual Reality Sickness Questionnaire (VRSQ) [87] was completed, which gives a score of motion sickness measurement index in virtual reality. None of the participants indicated any issues related to motion sickness.

2.3. Procedure

The experiment consisted of 4 repetitions of the sparkles workload-inducing paradigm, while participants' EEG data was recorded. The order of the conditions was decided randomly (2 by 2 conditions, hence 24 possible orders). The conditions were the following:

1. Computer screen modality and sitting posture (CS-sit);
2. VR modality and sitting posture (VR-sit);

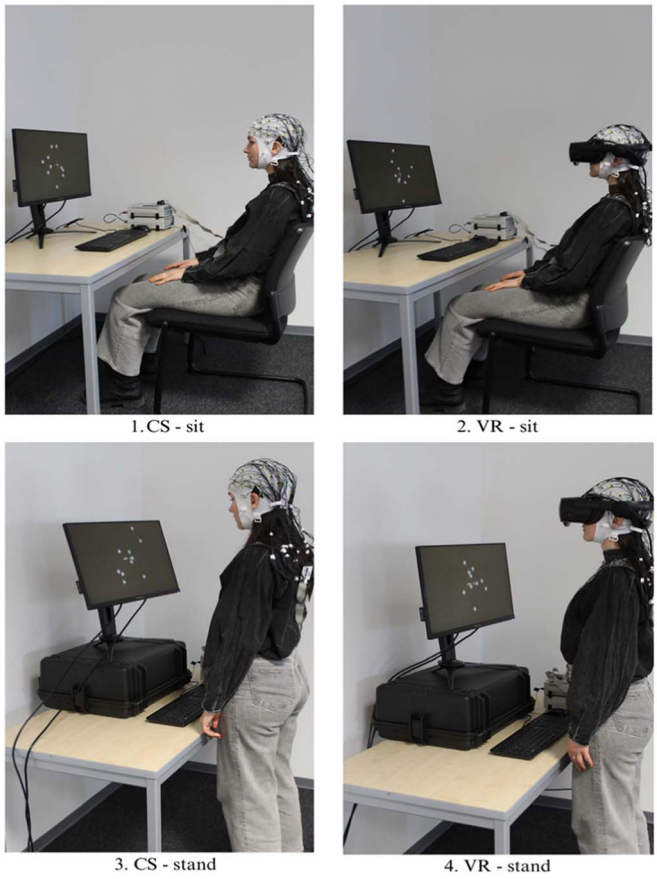

Figure 2. Experimental setup for the study's 4 conditions: CS-sit (Computer Screen, sitting), VR-sit (Virtual Reality, sitting), CS-stand (Computer Screen, standing), and VR-stand (Virtual Reality, standing).

3. Computer screen modality and standing posture (CS-stand);
4. VR modality and standing posture (VR-stand).

One task lasted for about 8 min. Each trial lasted 10 seconds, resulting in 200 seconds of EEG data per trial class in each condition. The overall experiment per participant, including consent, EEG preparation, VR familiarisation and self-paced breaks lasted about 2.5 h. Figure 2 displays the setup for each of the 4 conditions.

2.4. Data processing

2.4.1. Signal alterations

We processed the data in different ways to extract measures corresponding to the muscle activity hypothesis, the SNR hypothesis, the frontal rest theta and parietal rest alpha power, and the classification accuracies. Before these analyses, the raw EEG data was firstly pre-processed. We removed the non-experimental data segments such as EEG recorded during self-paced breaks between blocks. Then, we removed the noisy channels and filtered the data using a FIR forward-backward (non-causal) Kaiser filter at a 0.5 Hz cutoff edge. For this, we used the clean_artifacts EEGLAB function with a minimum channel correlation of 0.8 and a line noise criterion of 4. Afterward, we applied a spherical interpolation method and re-referenced the channels to a common average reference. Then, independent components were obtained with the AMICA algorithm [88]. To improve the decomposition, the automatic sample rejection parameters of AMICA were used, in line with [89]. Before each analysis, the obtained data was initially downsampled to 250 Hz. After these steps, the resulting datasets will be referred to as post-ICA datasets going further.

The EEGLAB [90] and BCILAB 1.4-devel [91] toolboxes integrated into MATLAB R2022a (The Mathworks, Inc., Natick, MA, USA) were used for EEG data analysis and BCI classification and training, respectively. RStudio [92] was used for statistical analyses.

2.4.2. Muscle activity

To test the muscle activity hypothesis, the independent components of the post-ICA datasets were automatically labelled with the ICLabel algorithm (version 1.4, default settings) [93]. After a dipole fitting using the DIPFIT plugin from EEGLAB, datasets containing only muscle components were generated by removing the non-muscle components after the automatic labelling. The data was further filtered with a FIR filter

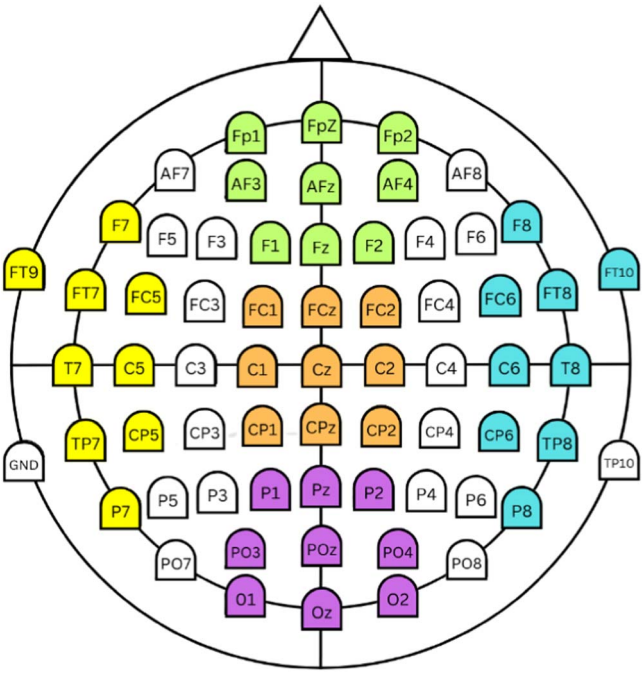

Figure 3. Channel selections for the frontal (green), central (orange), occipital (purple), temporal left (yellow), and temporal right (blue) in the muscle power analysis.

using a Hamming window to obtain the broadband signal (1–100 Hz passband edges). After segmenting the data in 1-second epochs, the log power spectral densities (log PSD) were computed using Welch's method [94] for 5 regions, each including 9 channels: frontal (Fp1,FpZ, Fp2, AF3, AFz, AF4, F1, Fz, F2), central (FC1, FCz, FC2, C1, Cz, C2, CP1, CPz, CP2), occipital (P1, Pz, P2, PO3, POz, PO4, O1, Oz, O2), temporal-left (FP9, F7, FT7, FC5, T7, C5, TP7, CP5, P7) and temporal-right (F8, FC6, FT8, FT10, C6, T8, CP6, TP8, P8). These region-specific selections of electrodes can be seen in figure 3. The final statistical analyses compared these log PSD values averaged across channels between the sit and stand posture conditions.

2.4.3. SNR

The presumed HMD-VR and standing posture impact on the EEG were examined by comparing the SNR values between the conditions. We operationalized SNR in two ways: the SNR corresponding to theta, and the SNR corresponding to alpha. Specifically, we averaged the variance of theta over all electrodes and the variance of alpha across all electrodes, according to the following equations:

$$SNR_{alpha} = \frac{mean(\mathrm{var}(alphaBand))}{mean(\mathrm{var}(broadBand))}$$

$$SNR_{theta} = \frac{mean(\mathrm{var}(thetaBand))}{mean(\mathrm{var}(broadBand))}$$

Before these calculations, the band varience values were obtained after applying corresponding bandpass FIR filters with a Hamming window for theta (4–7 Hz passband edges), alpha (8–13 Hz passband edges), and broadband (1–40 Hz passband edges) and then epoching the data in 1-second segments. The obtained SNR values were averaged across channels and epochs for each subject and each posture-modality combination. Then, these were statistically compared across conditions.

2.4.4. Signal of interest

To investigate the impact of posture and modality on the signal of interest, further processing steps were applied on the post-ICA datasets. The data was filtered with a bandpass FIR filter (1–100 Hz passband edges) using a Hamming window and then segmented in 1-second epochs for high workload and no workload trials, respectively. Then, the eye components were removed with the ICLabel algorithm. For the alpha-parietal brain region, 5 channels (Pz, P1, P2, CPz, and POz) were selected. Also, 5 channels (AFz, F1, Fz, F2, FCz) were chosen for the theta frontal region.

We operationalize the signal of interest as the rest (no workload) parietal alpha band and the rest (no workload) frontal theta. Thus, only *no workload* trials were selected for both the alpha and theta band activity investigation. These two frequency bands were analyzed separately to assess their individual contributions to cognitive workload and their response to different conditions. Log PSD values were obtained for each participant by averaging channel log PSD across all relevant electrodes for each condition and frequency band.

2.4.5. pBCI performance

For the binary classification of the recorded signal in high versus low workload, we used the post-ICA

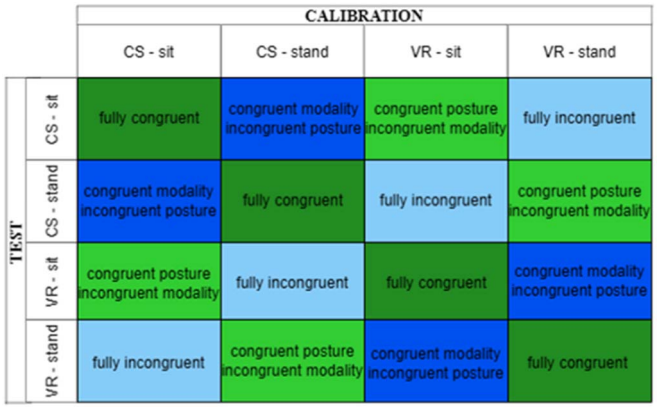

Figure 4. Level assignment logic to the cross-context condition variable.

datasets. Then, we identified the eye artifact components with the ICLabel and removed them with 15% residual variance after the automatic labelling. We applied the filter bank common spatial patterns (FBCSP) method [95] on the epoched data to obtain the features corresponding to the power in the theta (4–7 Hz) and alpha (8–13 Hz) frequency ranges. Linear discriminant analysis (LDA) with a 5-fold cross-validation repeated 5 times was used to separate the classes. The calibration data comprised the first 80% of the corresponding dataset. An online phase was simulated in an offline manner as well by applying the obtained model to the last 20% of each corresponding dataset. This cross-validation was performed exclusively on the calibration data. Going further, these will be referred to as *calibration* data and *test* data. This split was chosen to replicate a typical BCI application scenario where the system undergoes a distinct training (calibration) phase followed by a testing phase. The features used for the classification were 12 spatial filters for the FBCSP method. The *pBCI decoding performance* was estimated as the average classification accuracies obtained on the test data. These accuracies were then statistically compared between conditions.

2.4.6. Cross-context application performance

For the cross-context application analysis, we first trained a classifier on the calibration data of each subject and each condition using the same approach described in the previous section for the post-ICA datasets. Then, the resulting classifier was applied to the same subject's test data for each condition. For example, a classifier that was trained on the calibration data for the CS-sit condition for subject 1 would be applied to the same subject's test data for the conditions CS-sit, CS-stand, VR-sit, and VR-stand, sequentially. The same classification method as in the previous section was applied. In this case, we will name such data for 4 conditions the *cross-context test data*. We define here cross-context application performance as the average classification accuracy obtained on the cross-context test data. A new variable with 4 levels called *cross-context condition* was created, corresponding to each of the cross-context test accuracies. Depending on the calibration and testing condition pair, each accuracy value was assigned one of the following levels: fully congruent, fully incongruent, congruent modality & incongruent posture, congruent posture & incongruent-modality. More specifically, if the cross-context test data originated in the same modality condition and the same posture condition as the calibration data the classifier was obtained on, the cross-context condition level was set to fully congruent. Otherwise, if the cross-context test data originated in both a different modality and posture condition compared to the calibration data, the cross-context condition level was set to fully incongruent. If the cross-context test data originated in modality that is different from its calibration data, but the same posture, the cross-context condition level was set to congruent modality & incongruent posture. Lastly, if the cross-context test data originated in modality that is different from its calibration data, but the same posture, the cross-context condition level was set to congruent posture & incongruent modality. Figure 4 illustrates this logic. The cross-context condition variable was subsequently used in statistical analyses as an independent variable.

2.5. Statistical analyses

The investigation on muscle activity employed a comparison between the sitting and standing posture for 5 channel regions with t-tests after a normality assumption inspection. For signal analyses and pBCI decoding performance tests we performed two-way analyses of variance with interactions (2×2 factorial repeated-measures ANOVA). The two-way ANOVAs were built to assess posture and modality's impact on each described dependent variable (average SNRs, signals of interest and pBCI decoding performance). Prior to performing the analyses, the assumptions of two-way ANOVAs were checked. The residual normality assumption was visually inspected through QQ plots. For the cross-context application performance

analysis, the cross-context condition variable was used as an independent factor in a one-way repeated-measures ANOVA model to predict the cross-context test accuracies. If main effects were found to be statistically significant, estimated marginal means with Bonferroni adjustment were used to perform post-hoc pairwise comparisons. To further investigate the equivalence of groups when no significant main effect or no significant differences were found, the two-one sided tests (TOST) [96] procedure was applied for all investigated analyses. A p-value of 0.05 was chosen as the significant threshold for all TOST analyses. As the CS-sit condition was considered to represent the control condition, we chose an epsilon of the standard deviation of the corresponding measures obtained in this condition. Therefore, the standard deviation of the mean muscle power in CS-sit, the standard deviation of the mean rest alpha and theta power in CS-sit, the standard deviation of the mean alpha SNR and theta SNR in CS-sit, and the standard deviation of the pBCI accuracies in CS-sit were chosen as epsilon values for each corresponding analysis case.

3. Results

3.1. Signal alterations results

3.1.1. Muscle activity

A paired t-test was performed to compare the band power between the sit and stand condition for each of the 5 channel regions, with the hypothesis that the band power in the standing posture was significantly greater than in the sitting posure. For the occipital region, the results indicated that the band power in the standing posture ($M = -3.977$, $SD = 8.810$) is greater than the bandpower in the sitting posture ($M = -4.549$, $SD = 8.608$) ($p = .041$). The muscle bandpower in the standing posture ($M = -5.440$, $SD = 5.723$) was not greater than bandpower in the sitting condition ($M = -5.431$, $SD = 6.159$) ($p = .507$) for the frontal region. The TOST procedure with an epsilon of the standard deviation of this channel region's CS-sit mean muscle power revealed that the sit and stand mean muscle power groups are equivalent (mean difference $= 0.009$, epsilon $= 6.375$, $p < .001$) in the frontal region. Also, the muscle bandpower in the standing posture ($M = -7.091$, $SD = 8.195$) was not greater than bandpower in the sitting condition ($M = -7.364$, $SD = 7.919$) ($p = .176$) for the central region. The TOST procedure with an epsilon of the standard deviation of the central region's CS-sit mean muscle power revealed that the sit and stand mean muscle power groups are equivalent (mean difference $= -0.273$, epsilon $= 7.970$, $p < .001$) in the central region. Similarly, the muscle bandpower in the standing posture ($M = -1.431$, $SD = 6.341$) was not greater than bandpower in the sitting condition ($M = -1.843$, $SD = 6.678$) ($p = .18$) for the temporal right region. According to the TOST procedure with an epsilon of the standard deviation of the temporal right region's CS-sit mean muscle power, the sit and stand mean muscle power groups are equivalent (mean difference $= -0.411$, epsilon $= 7.367$, $p < .001$) in the temporal right region. Lastly, the muscle bandpower in the standing posture ($M = -1.431$, $SD = 6.341$) was not greater than bandpower in the sitting condition ($M = -1.834$, $SD = 6.678$) ($p = .18$) for the temporal left region. The TOST procedure using an epsilon of the CS-sit mean muscle power standard deviation in the temporal left region showed that the sit and stand mean muscle power groups are equivalent (mean difference $= -0.283$, epsilon $= 6.740$, $p < .001$) in the temporal left region.

3.1.2. SNR

The first ANOVA test revealed no significant main effect of modality on alpha SNR values, $F(1, 21) = 1.181$, $p = .289$. Two TOST procedures with an epsilon of the standard deviation of the alpha SNR in the CS-sit condition were conducted for the CS and VR modality sub-groups within the sit and stand groups. Within the sit condition, the CS and VR alpha SNR groups are equivalent (mean difference $= -0.002$, epsilon $= 0.041$, $p < .001$). Within the stand condition, the CS and VR alpha SNR groups are also equivalent (mean difference $= -0.010$, epsilon $= 0.041$, $p < .001$). Similarly, posture did not exhibit a significant main effect, $F(1, 21) = 9.55$, $p = .289$. Another two TOST procedures with an epsilon of the standard deviation of the alpha SNR in the CS-sit condition were conducted for the sit and stand posture sub-groups within the CS and VR groups. Within the CS condition, the sit and stand alpha SNR groups are equivalent (mean difference $= 0.010$, epsilon $= 0.041$, $p < .001$). Within the VR condition, the sit and stand alpha SNR groups are also equivalent (mean difference $= 0.002$, epsilon $= 0.041$, $p < .001$). The interaction between modality and posture was also not significant, $F(1, 21) = 0.602$, $p = .447$. Hence, the alpha SNR values do not significantly differ across levels of modality or posture, and there is no significant interaction between these two factors when it comes to alpha-specific signal-to-noise-ratios.

The second ANOVA test yielded a main significant effect of the modality for theta SNR values, $F(1,21) = 5.311$, $p = .031$. A post hoc pairwise comparison of the marginal means with Bonferroni adjustment revealed that the theta SNR for the CS modality ($M = 0.157$, $SD = 0.040$) is significantly higher than for the VR modality ($M = 0.144$, $SD = 0.037$) ($p = .031$). Posture did not have a significant main effect at the level of theta SNR, $F(1,21) = 1.415$, $p = .248$, nor did the interaction between modality and posture, $F(1,21) = 3.845$, $p = .063$. Two TOST procedures with an epsilon of the standard deviation of the theta SNR in the CS-sit condition were conducted for the sit and stand posture sub-groups within the CS and VR groups. Within the CS condition, the sit and stand theta SNR groups are

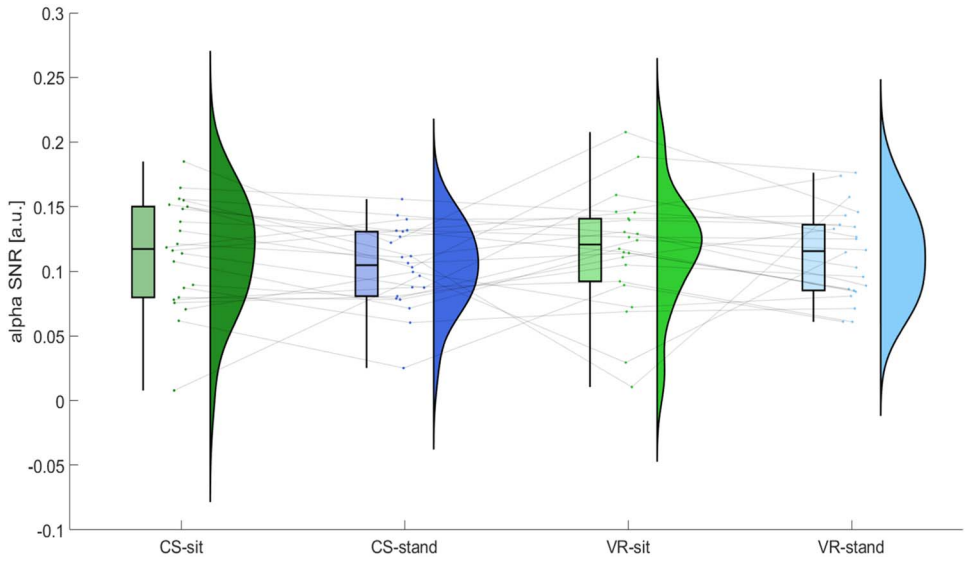

Figure 5. Data distributions of alpha Signal-to-Noise Ratio (SNR) values for the four conditions. Connected points across conditions represent paired measurements from the same subjects.

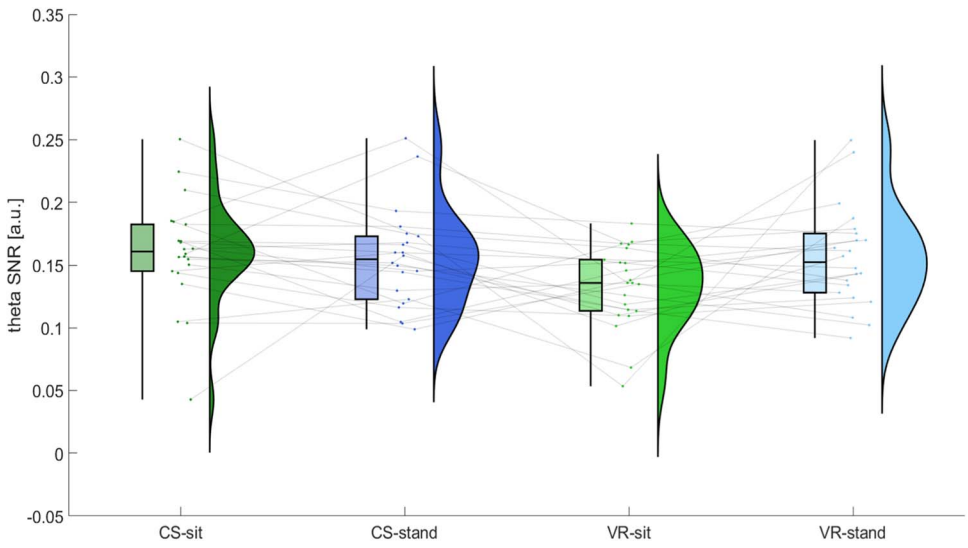

Figure 6. Data distributions of theta Signal-to-Noise Ratio (SNR) values for the four conditions. Connected points across conditions represent paired measurements from the same subjects.

equivalent (mean difference = 0.005, epsilon = 0.042, $p < .001$). Within the VR condition, the sit and stand theta SNR groups are not equivalent (mean difference = −0.023, epsilon = 0.042, $p = .058$). The distribution of the alpha SNR and theta SNR values is illustrated in figures 5 and 6, respectively.

3.1.3. Signal of interest

To ensure the validity of the neurophysiological effects of the workload-inducing paradigm, topographical plots of the theta (4–8 Hz) and alpha (8–13 Hz) band activity were generated across subjects, conditions, and workload levels, which allowed for the visual inspection of the spectral power distributions. Figure 7 illustrates these topographical plots. In this figure, a frontal increase in the theta level and a parietal decrease in the alpha level can be observed during high workload, as expected. Averaged event-related spectral perturbation (ERSP) plots for Fz and Pz channels across 10s trials further confirm these neurophysiological effects for all conditions (figure 8). Statistical tests were conducted to investigate differences in band power between conditions. The theta band powers for resting state (no workload) trials represented the dependent variable in a first two-way factorial ANOVA. Our analyses found no main effect of posture ($F(1, 21) = 0.028$, $p = .869$). Two TOST procedures with an epsilon of the standard deviation of the theta rest power in the CS-sit condition were conducted for the sit and stand posture sub-groups within the CS and

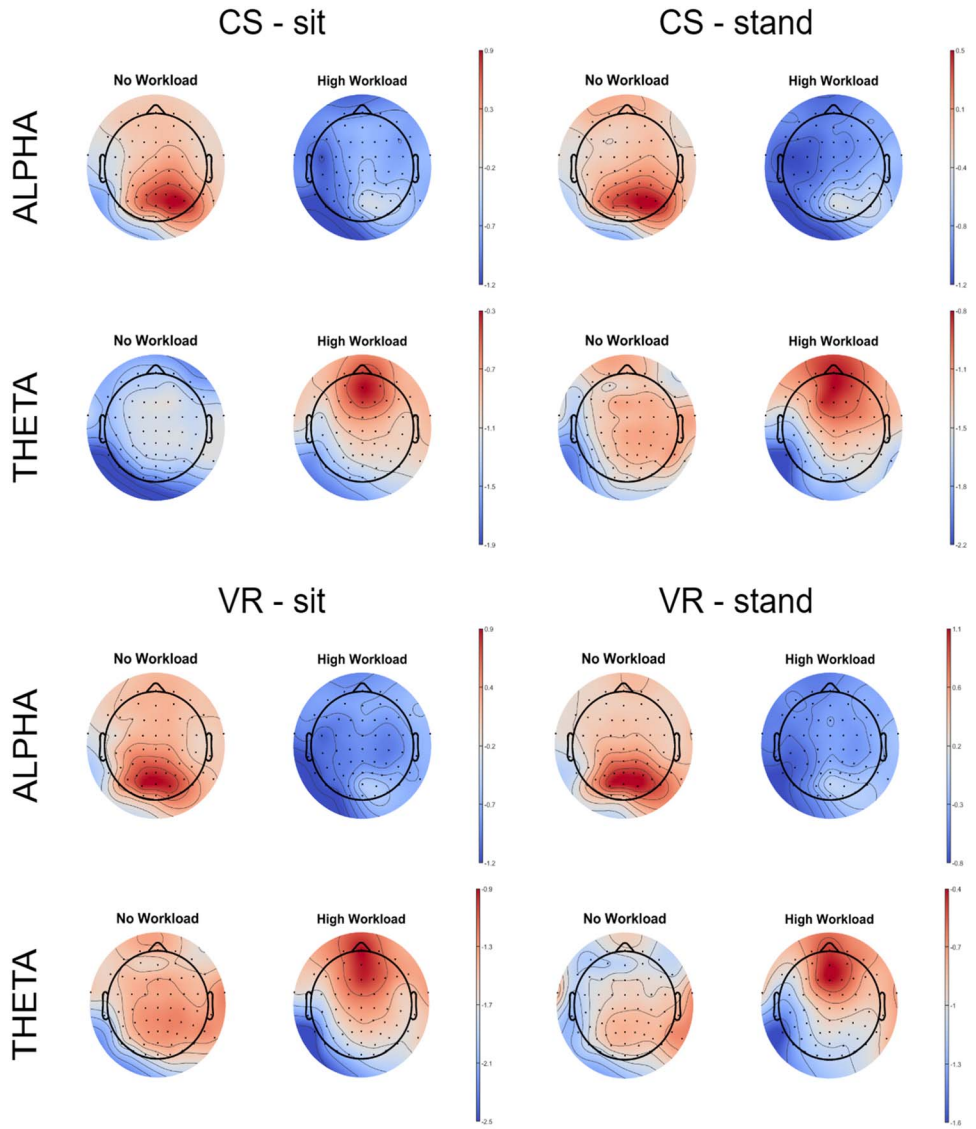

Figure 7. Scalp topographical maps illustrating the alpha (top rows) and theta (bottom rows) power for 'no workload' and 'high workload' trials averaged across time, trials and subjects for the four experimental setups.

VR groups. Within the CS condition, the sit and stand rest theta power groups are equivalent (mean difference = −0.334, epsilon = 2.458, $p < .001$). Within the VR condition, the sit and stand rest theta power groups are also equivalent (mean difference = 0.468, epsilon = 2.458, $p < .001$). However, a main significant effect of modality was found ($F(1, 21) = 15.11$, $p < .001$). A post hoc pairwise comparison of the marginal means with Bonferroni adjustment confirmed that the rest theta band power for the CS modality (M = 6.842, SD = 2.455) is significantly higher than for the VR modality (M = 6.034, SD = 2.391) ($p < .001$). The interaction between modality and posture was not significant ($F(1, 21) = 2.07$, $p = .165$).

A second ANOVA test was conducted for the resting state (no workload) alpha band power. There was no significant main effect of posture ($F(1, 21) = 0.35$, $p = .56$). Two TOST procedures with an epsilon of the standard deviation of the alpha rest power in the CS-sit condition were performed for the sit and stand posture sub-groups within the CS and VR groups. Within the CS condition, the sit and stand rest alpha power groups are equivalent (mean difference = −0.112, epsilon = 3.413, $p < .001$). Within the VR condition, the sit and stand rest alpha power groups are also equivalent (mean difference = 0.523, epsilon = 3.413, $p < .001$). There was also no significant main effect of modality ($F(1, 21) = .193$, $p = .665$) or, posture-modality interaction ($F(1, 21) = 1.125$, $p = .301$) on rest alpha bandpower. Another two TOST procedures with an epsilon of the standard deviation of the alpha rest power in the CS-sit condition were conducted for the CS and VR modality sub-groups within the sit and VR stand groups. Within the sit condition, the CS and VR rest alpha power groups are equivalent (mean difference = −0.448, epsilon = 3.413, $p < .001$). Within the VR condition, the sit and stand rest alpha power

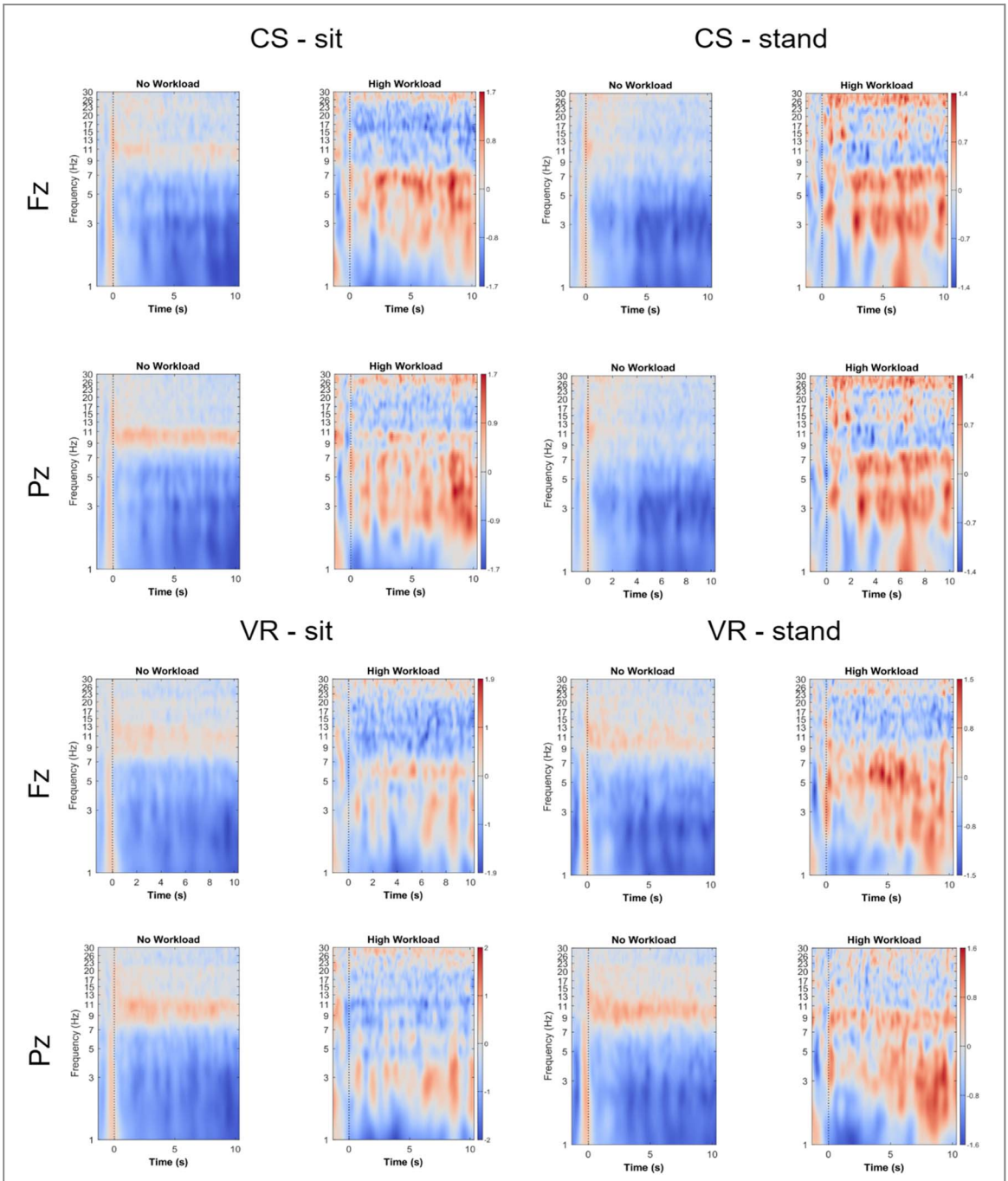

Figure 8. Time-frequency representations of the EEG data at Fz and Pz channels for 'no workload' and 'high workload' averaged across subjects and the 10-second trials for the four experimental setups.

groups are also equivalent (mean difference = 0.186, epsilon = 3.413, $p < .001$).

3.2. pBCI decoding performance results

Table 1 reports the average accuracies obtained on the test data for each condition. According to the ANOVA test, there were no main effects of posture ($F(1, 21) = 0.042$, $p = .839$).

Two TOST procedures with an epsilon of the standard deviation of the test accuracies in the CS-sit condition were conducted for the sit and stand posture sub-groups within the CS and VR groups. Within the CS condition, the sit and stand pBCI accuracy groups are equivalent (mean difference = −0.021, epsilon = 0.099, $p < .001$). Within the VR condition, the sit and stand pBCI accuracy groups are also equivalent

Table 1. pBCI decoding performance metrics.

Condition	Test TP (%)	Test TN (%)	Test accuracy (%)
CS - sit	72	71	71
CS - stand	75	73	74
VR - sit	76	73	74
VR - stand	71	72	72

TP = True positives; TN = True negatives

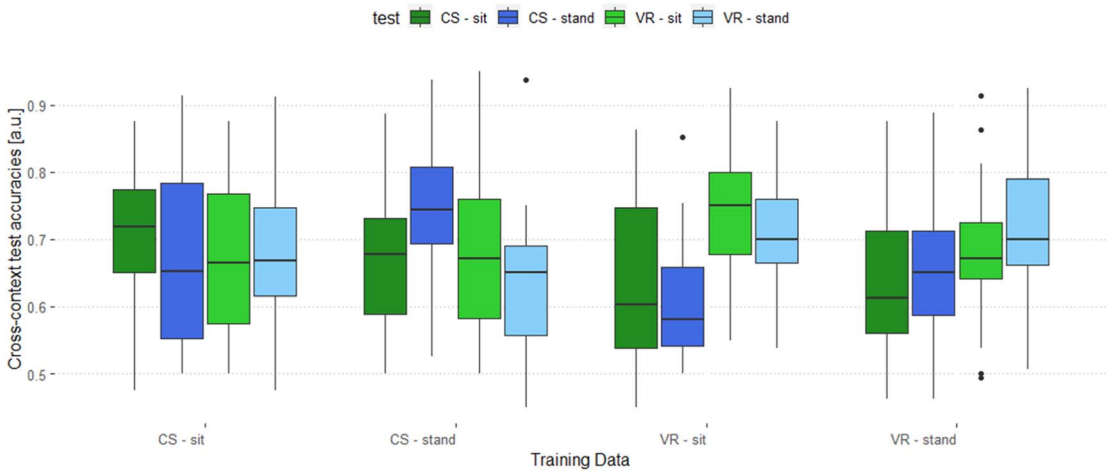

Figure 9. Cross-context application performance (i.e. average accuracies) obtained across all conditions. Each boxplot shows the distribution of accuracies when the classifier, trained in a specific condition (indicated on the x-axis), is tested on different conditions (color-coded categories).

(mean difference = 0.028, epsilon = 0.099, $p = .003$). The main effect of modality ($F(1,21) = 0.05$, $p = .826$) or posture-modality interaction ($F(1, 21) = 2.311$, $p = .143$) at the level of average pBCI accuracies were also not significant. Two TOST procedures with an epsilon of the standard deviation of the test accuracies in the CS-sit condition were conducted for the CS and VR modality sub-groups within the sit and stand groups. Within the sit condition, the CS and VR pBCI accuracy groups are equivalent (mean difference = −0.028, epsilon = 0.099, $p = .002$). Within the stand condition, the CS and VR pBCI accuracy groups are also equivalent (mean difference = 0.021, epsilon = 0.099, $p = .001$). Hence, the pBCI accuracies are not significantly different across the levels of modality and posture and there is no significant interaction between these two factors.

3.3. Cross-context application performance results

The overall average cross-context application performance across conditions is shown in figure 9. The cross-context application performance (M = 0.659, SD = 0.114) was decreased in comparison with the average pBCI decoding performance reported in the above section (M = 0.728, SD = 0.104). The one-way repeated measures ANOVA model revealed a statistically significant effect for the cross-context condition ($F(3, 63) = 23$, $p < .001$). A post hoc pairwise comparison of the marginal means with Bonferroni adjustment led to significant differences between the condition groups. The fully congruent condition (M = 0.728, SD = 0.105) yielded significantly higher accuracy compared to the fully incongruent condition (M = 0.650, SD = 0.115) ($p < .001$), the congruent posture & incongruent modality condition (M = 0.648, SD = 0.117) ($p < .001$), and the congruent modality & incongruent posture condition (M = 0.680, SD = 0.111) ($p < .001$). Additionally, the congruent modality & incongruent posture condition (M = 0.680, SD = 0.111) led to significantly higher accuracy compared to the fully incongruent condition (M = 0.650, SD = 0.115) ($p = .04$) and the congruent posture & incongruent modality condition (M = 0.648, SD = 0.117) ($p = .03$). There was no significant difference between the fully incongruent (M = 0.650, SD = 0.115) and congruent posture & incongruent modality (M = 0.648, SD = 0.117) condition ($p = .99$).

The TOST analysis revealed that the fully incongruent and congruent posture & incongruent modality cross-context accuracy groups are equivalent (mean difference = −0.03, epsilon = 0.099, $p < .001$). These results suggest that better workload decoding can be achieved in a new context, if the classifier is trained on data recorded within the same condition. Figure 10 depicts these findings.

3.4. Summary of significant results

To facilitate clarity and provide a concise overview of the key findings, table 2 summarizes the statistically significant differences observed across the different analyses.

4. Discussion

4.1. Overview

Passive BCIs have tremendous potential for real-life application, enabling new ways of human-machine communication–if they can be meaningfully deployed in real-life contexts. With our study, we intended to provide new insights into the contextual feasibility of pBCI by studying the effect of modality- and posture-related variations in the signal and classifier performance, as these two dimensions are highly relevant to real-life applicability.

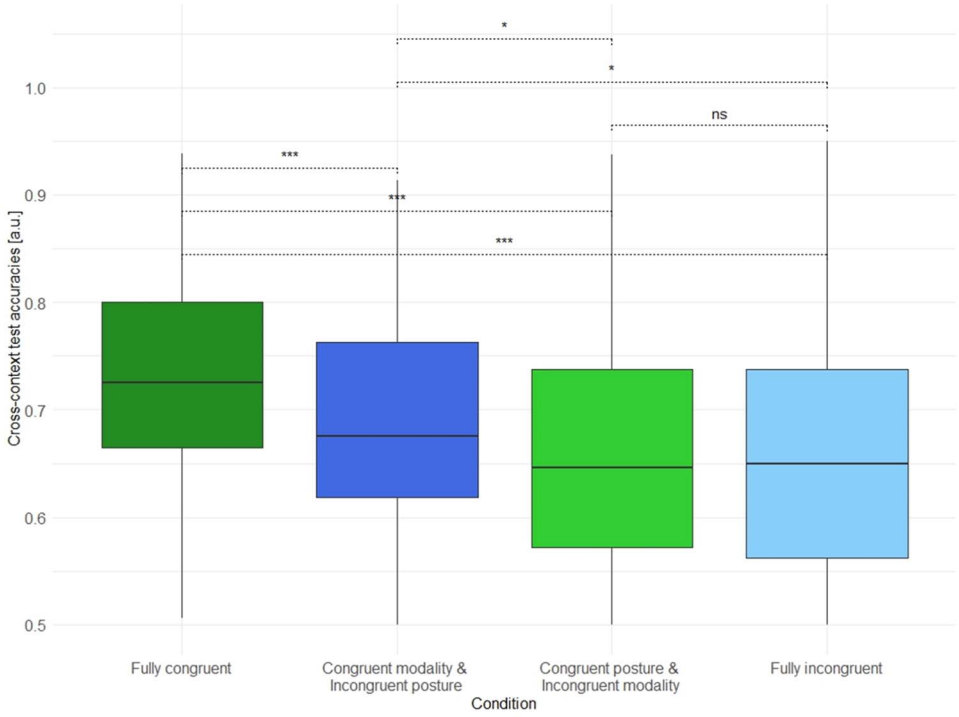

Figure 10. Cross-context test accuracies of pBCI classifiers under different posture and modality congruency conditions. Fully congruent conditions show the highest accuracy, while accuracy drops when posture or modality becomes incongruent. There is no significant difference ('ns') between fully incongruent and congruent posture/incongruent modality. Statistical significance is marked by $^{*}p < 0.05$, $^{**}p < 0.01$, $^{**}p < 0.001$.

Table 2. Significant differences found between groups for each analysis.

Analysis	Comparison	P-value
Muscle activity	standing Versus sitting (occipital region)	$p = .041$
Theta SNR	CS Versus VR	$p = .031$
Frontal rest theta power	CS Versus VR	$p < .001$
Cross-context application Performance	fully congruent Versus fully incongruent	$p < .001$
	fully congruent Versus congruent modality & incongruent posture	$p < .001$
	fully congruent Versus congruent posture & incongruent modality	$p < .001$
	fully incongruent Versus congruent modality & incongruent posture	p = .04
	fully incongruent Versus congruent posture & incongruent modality	p = .03

Does the modality of task presentation or posture affect the power in the rest alpha and rest theta frequency bands, the signal-to-noise ratio and muscle activity?

Our results indicate that the EEG signals relevant for a workload classifier are partly altered by posture and by the modality of task presentation. More specifically, we observed more muscle artifacts present when the task was completed in an upright posture, as opposed to a sitting posture in one of the 5 investigated channel regions, the occipital region. Observing more muscle activity in an upright posture is consistent with the muscle argument and in line with studies that found an increased electromyography (EMG) activity in the trunk when standing standing, compared to sitting postures [97, 98] or particular changes in the EEG signal in the occipital region during when standing up [27, 33].

Posture did not appear to have a significant effect on the parietal rest alpha and frontal rest theta, our signals of interest. These observations are in contrast with some prior analyses that found neurophysiological differences between different postural conditions [33, 34], but is not entirely suprising given that the experimental design did not involve significant physical movement. However, we found that the modality of task presentation had a significant effect on the frontal rest theta power.

Similarly, the modality had a significant main effect on the theta SNR, corroborating findings from previous studies that looked at the impact of HMD-VR on EEG and found variations at the level of the signal [71]. Nevertheless, this finding is noteworthy given that the additional disturbance brought by HMD-VR usually alters higher frequencies (above 50 Hz)

[69, 93]. This effect was not found at the level of alpha SNR. In line with the results on the rest alpha and theta power, posture did not significantly change the theta SNR or alpha SNR. In short, our first set of hypotheses on the impact of standing posture and HMD-VR headsets was partially confirmed.

Does the modality of task presentation or posture matter for the pBCI's ability to decode mental states?

Although analyzing the signal changes across conditions was an important prerequisite to understanding how these variations can affect the pBCI classification, our main focus was to investigate if pBCIs remain robust in unconventional situations. According to our results, the calibration algorithm is not significantly influenced by the signal variations, and no significant differences in classification capabilities were found between conditions. Hence, the second set of hypotheses stating that the pBCI performance in workload detection will be affected by the potential EEG alterations was not confirmed.

These results are in line with other studies that investigated the feasibility of decoding mental states in standing conditions for reactive BCI [41] or active BCI [40], but there is no prior research involving a comparative analysis for pBCI in different postures. A case study on the feasibility of MI-BCI in sitting and standing, which found that despite different EEG patterns occurring between the two postures, imagined hand movement classification is possible in both [40]. Our results are also in line with a study that assessed how a P300-based BCI performs with stimuli presented in augmented reality (AR) across 3 postural settings (sitting, standing, and walking in place) [99]. According to the author's analysis, the area amplitude and latency of the P300 and N200 components did not change with posture, indicating that P300-based BCIs might be suitable for diverse postural conditions. In comparison to such studies that focused on active and reactive BCIs, the present investigation explored the distinct signals relevant for pBCIs in the face of changes in context (posture and modality). Our findings provide a hopeful perspective for the usability of BCIs in general, and specifically for the feasibility of pBCIs for gaming, work settings and leisure activities.

How well can classifiers generalize across body posture and stimulus presentation modality conditions?

Significant effort has been put lately into solving the problem of generalization for BCIs [100]. Here we investigated transfer learning in a new way. Instead of task-/session- or subject independence, we looked at how a pBCI workload classifier can generalize across different context changes in terms of body posture or presentation modality. We observed that changes to the modality or posture conditions lead to a decrease in accuracy, while the best test classifier performance is achieved when the modality and posture conditions are kept constant. The classification is particularly impacted when both modality and posture differ from the training conditions. The non-significant difference between the fully incongruent and congruent posture & incongruent modality conditions indicates that keeping the posture congruent doesn't significantly boost the classifier accuracy when modality is incongruent. These results also match the findings obtained for the EEG signal, where the modality factor had a significant effect on the frontal rest theta power and theta SNR. For practical applications that require a high level of accuracy, this finding could suggest that ensuring consistency for the task presentation modality might bring more advantages to the pBCI performance, compared to body posture consistency. Confirming our third hypothesis, the results indicate one should be aware of potential drops in accuracy if the mental state classification model was trained on data recorded in a different modality or posture, but the decoding can still be achieved in a relatively robust way. Improvements for cross-context transfer might come from research on domain adaptation that aims to resolve the disparity in EEG signal distribution across conditions through methods such as one-to-one and many-to-one transfer schemes [101].

4.2. Limitations and future directions

Our investigation on postural differences is limited to only two static postures, while there exists a broad range of positions a pBCI user might find themselves in. A deeper understanding of the technology's feasibility in real contexts would require a more in-depth analysis of how pBCI performs in various body movements. Recent MoBI studies have looked at the brain dynamics and natural cognition in active states such as walking in real [102] or virtual [103] environments. While classification has been investigated during walking for reactive BCI [104], it remains to be seen if pBCI can be reliably used in movement-prone situations. Given a surge in interest in VR and BCI synergy, it would be especially interesting to expand the pBCI-HMD-VR research to study the capabilities of dynamic immersive games or tasks that make use of pBCIs.

While our study eases some of the common concerns associated with respect to the interference of the equipment [55] in such pBCI-HMD-VR research and applications, the results were obtained on average SNR metrics across all channels, for the specific case of gel electrodes. Despite a persistent lack of trust in non-gel electrodes in EEG laboratories [105], an improved signal-to-noise ratio in newer devices was observed [18, 106, 107] and some proof that pBCIs can operate adequately with dry electrodes even under less controlled conditions [108]. Standard high-density dry electrodes solve the problem of a lengthy application process to the scalp, but the trade-off in signal quality and rapid decline in comfort due to friction and pressure to the head [109] make them unsuitable candidates for VR displays for now. With the surge in interest for both BCI and VR, a lot of engineering

effort is currently put into creating more user-friendly equipment [18]. Also, more sparse, dorsal electrode layouts could be suitable for EEG recordings and analysis and might offer solutions to the problem of VR interference [110]. In recent years, around-the-ear electrodes (cEEGgrids) have been manufactured and tested [111]. These could be viable and more user-friendly alternatives for brain electrical activity recording, as well as better suited to combine with VR devices, eliminating the problem of added pressure. Hence, our findings represent a preliminary view into the feasibility of the pBCI-VR combination, but more research is needed to explore other electrode density types (e.g. 64 electrodes Versus 16 electrodes), electrode positioning (e.g. on scalp Versus around the ears) and electrode interface types (e.g. gel Versus dry). Such additional studies might help the field to find a good balance between decoding performance, cost, and ease of use and propel pBCI into more practical settings. Moreover, the present methods were intended to simulate an online scenario, with the assumption that the obtained results would also be suitable for real-time classification. Still, we chose to remove the eye components from the signal with AMICA, which is too computationally demanding to fit the timing constraints of online scenarios. Instead, a more suitable version of ICA might be ORICA [112]. These findings may also not generalize to pBCI classifiers that are trained with other feature types. For instance, more work is needed to understand if pBCIs based on time-domain features or time-frequency domain features remain robust across variations in contexts.

5. Conclusions

This study is a step forward to a better understanding of pBCIs' applicability to real-world scenarios, specifically when users are more mobile and may be using VR. Despite some alterations in signal and cross-context performance, we found that the task presentation modality and subject posture did not significantly impact the ability of a classifier to decode mental state information.

Acknowledgments

The authors thank Dr Theodor-Solis Escalante for his assistance with the EEG analysis. We also are grateful to Maria Faragau for her help with recording the data.

Data availability statement

The data cannot be made publicly available upon publication because they contain sensitive personal information. The data that support the findings of this study are available upon reasonable request from the authors.

Ethical statement

Ethics approval was obtained through Brandenburg University of Technology Cottbus-Senftenberg (BTU CS) ethics committee EK2022–3.

Funding

This study was supported by the Volkswagen Foundation by funding the Lichtenberg Professorship Neuroadaptive Human-Computer Interaction at BTU CS.

ORCID iDs

Diana E Gherman https://orcid.org/0000-0002-9119-0473
Laurens R Krol https://orcid.org/0000-0002-6585-2795
Marius Klug https://orcid.org/0000-0001-8667-3457
Thorsten O Zander https://orcid.org/0000-0003-3111-2470

References

[1] Zander T O 2008 Enhancing human-machine systems with secondary input from passive brain-computer interfaces *In: Proceeding of 4th Internatinal BCI Workshop* 44–9
[2] Zander T O and Kothe C 2011 Towards passive brain-computer interfaces: applying brain-computer interface technology to human-machine systems in general *J. Neural Eng.* **8** 025005
[3] Pawlitzki J, Klaproth O, Krol L R and Zander T O 2021 Automation surprise in the neuroadaptive cockpit *In Proceedings of the 3rd International Neuroergonomics Conference (NEC)* **2021**
[4] Gerjets P, Walter C, Rosenstiel W, Bogdan M and Zander T O 2014 Cognitive state monitoring and the design of adaptive instruction in digital environments: lessons learned from cognitive workload assessment using a passive brain-computer interface approach *Front. Neurosci.* **8** 385
[5] Andreessen L M, Gerjets P, Meurers D and Zander T O 2021 Toward neuroadaptive support technologies for improving digital reading: a passive BCI-based assessment of mental workload imposed by text difficulty and presentation speed during reading *User Model. User-Adapt. Interact.* **31** 75–104
[6] Parra L C, Spence C D, Gerson A D and Sajda P 2003 Response error correction–a demonstration of improved human-machine performance using real-time EEG monitoring *IEEE Trans. Neural Syst. Rehabil. Eng.* **11** 173–7
[7] Grissmann S, Faller J, Scharinger C, Spüler M and Gerjets P 2017 Electroencephalography based analysis of working memory load and affective valence in an N-back task with emotional stimuli *Front. Hum. Neurosci.* **11** 616
[8] Krol L R and Zander T O 2022 chapter 2 - Defining neuroadaptive technology: the trouble with implicit human-computer interaction *Current Research in Neuroadaptive Technology* ed S H Fairclough and T O Zander (Academic) 17–42
[9] Andujar M and Gilbert J E 2013 *Let's learn! enhancing user's engagement levels through passive brain-computer interfaces CHI '13 Extended Abstracts on Human Factors in Computing Systems CHI EA '13* (Association for Computing Machinery) 703–8
[10] Lin C-T, Wu R-C, Liang S-F, Chao W-H, Chen Y-J and Jung T-P 2005 EEG-based drowsiness estimation for safety driving using independent component analysis *IEEE Trans. Circuits Syst. I Regul. Pap.* **52** 2726–38

[11] Zander T O et al 2017 Evaluation of a dry EEG system for application of passive brain-computer interfaces in autonomous driving *Front. Hum. Neurosci.* **11** 78
[12] Dehais F, Dupres A, Di Flumeri G, Verdiere K, Borghini G, Babiloni F and Roy R 2018 Monitoring pilot's cognitive fatigue with engagement features in simulated and actual flight conditions using an hybrid fNIRS-EEG passive BCI *2018 IEEE international conference on systems, man, and cybernetics (SMC)* (IEEE) 544–9
[13] Klaproth O W, Vernaleken C, Krol L R, Halbruegge M, Zander T O and Russwinkel N 2020 Tracing pilots' situation assessment by neuroadaptive cognitive modeling *Front. Neurosci.* **14** 795
[14] Gauba H, Kumar P, Roy P P, Singh P, Dogra D P and Raman B 2017 Prediction of advertisement preference by fusing EEG response and sentiment analysis *Neural Netw.* **92** 77–88
[15] Krol L R, Freytag S-C and Zander T O 2017 Meyendtris: a hands-free, multimodal tetris clone using eye tracking and passive BCI for intuitive neuroadaptive gaming *Proceedings of the 19th ACM International Conference on Multimodal Interaction ICMI '17: International Conference On Multimodal Interaction* (ACM)
[16] George L and Lécuyer A 2010 An overview of research on 'passive' brain-computer interfaces for implicit human-computer interaction *In Int. Conf. on Applied Bionics and Biomechanics ICABB 2010-Workshop W1 'Brain-Computer Interfacing and Virtual Reality'*
[17] Zabcikova M, Koudelkova Z, Jasek R and Lorenzo Navarro J J 2022 Recent advances and current trends in brain-computer interface research and their applications *Int. J. Dev. Neurosci.* **82** 107–23
[18] Niso G, Romero E, Moreau J T, Araujo A and Krol L R 2023 Wireless EEG: a survey of systems and studies *Neuroimage* **269** 119774
[19] Vázquez-Guardado A, Yang Y, Bandodkar A J and Rogers J A 2020 Recent advances in neurotechnologies with broad potential for neuroscience research *Nat. Neurosci.* **23** 1522–36
[20] Aricò P, Borghini G, Di Flumeri G, Sciaraffa N and Babiloni F 2018 Passive BCI beyond the lab: current trends and future directions *Physiol. Meas.* **39** 08TR02
[21] Roy R N and Frey J 2016 Neurophysiological Markers for Passive Brain-Computer Interfaces *Brain–Computer Interfaces 1: Foundations and Methods* 1 (Wiley) 85–100
[22] van Erp J, Lotte F and Tangermann M 2012 Brain-computer interfaces: beyond medical applications *Computer* **45** 26–34
[23] Zhang X, Krol L R and Zander T O 2018 Towards task-independent workload classification: Shifting from binary to continuous classification *IEEE Int. Conf. on Systems, Man, and Cybernetics (SMC)* (IEEE) 556–61
[24] Klosterman S L, Estepp J R, Monnin J W and Christensen J C 2016 Day-to-day variability in hybrid, passive brain-computer interfaces: comparing two studies assessing cognitive workload *Conf. Proc. IEEE Eng. Med. Biol. Soc.* **2016** 1584–90
[25] Wronkiewicz M, Larson E and Lee A K C 2015 Leveraging anatomical information to improve transfer learning in brain–computer interfaces *J. Neural Eng.* **12** 046027
[26] Mühl C, Jeunet C and Lotte F 2014 EEG-based workload estimation across affective contexts *Front. Neurosci.* **8** 114
[27] Thibault R T, Lifshitz M, Jones J M and Raz A 2014 Posture alters human resting-state *Cortex* **58** 199–205
[28] Zhong Z and Luo M 2021 Study on different postures based on EEG signals study on different postures based on EEG signals *2nd Int. Seminar on Artificial Intelligence, Networking and Information Technology (AINIT)* 169–74
[29] Ramadoss J, Dawi N M, Rajagopal K and Namazi H 2022 Complexity and information-based analysis of the electroencephalogram (EEG) signals in standing, walking, and walking with a brain–computer interface *Fractals* **30** 2250041
[30] Gramann K, Ferris D P, Gwin J and Makeig S 2014 Imaging natural cognition in action *Int. J. Psychophysiol.* **91** 22–9
[31] Jungnickel E, Gehrke L, Klug M and Gramann K 2019 Chapter 10 - MoBI—Mobile Brain/Body Imaging *Neuroergonomics* ed , F Ayaz and Dehais (Academic Press) 59–63
[32] Chen Y, Tang J H, Shou G, Gleghorn D, Doudican B C, Besio W, Cha Y-H, Ding L and Yuan H 2018 Effect of body positions on EEG signals in Mal de Debarquement Syndrome *Conf. Proc. IEEE Eng. Med. Biol. Soc.* **2018** 1931–4
[33] Zhavoronkova L A, Zharikova A V, Kushnir E M and Mikhalkova A A 2012 EEG markers of upright posture in healthy individuals *Hum. Physiol.* **38** 604–12
[34] Chang L-J, Lin J-F, Lin C-F, Wu K-T, Wang Y-M and Kuo C-D 2011 Effect of body position on bilateral EEG alterations and their relationship with autonomic nervous modulation in normal subjects *Neurosci. Lett.* **490** 96–100
[35] Tortora S, Artoni F, Tonin L, Chisari C, Menegatti E and Micera S 2020 Discrimination of walking and standing from entropy of EEG signals and common spatial patterns *2020 IEEE Int. Conf. on Systems, Man, and Cybernetics (SMC)* 2008–13
[36] Rice J K, Rorden C, Little J S and Parra L C 2013 Subject position affects EEG magnitudes *Neuroimage* **64** 476–84
[37] Mikkonen M and Laakso I 2019 Effects of posture on electric fields of non-invasive brain stimulation *Phys. Med. Biol.* **64** 065019
[38] Lifshitz M, Thibault R T, Roth R R and Raz A 2017 Source localization of brain states associated with canonical neuroimaging postures *J. Cogn. Neurosci.* **29** 1292–301
[39] Triana-Guzman N, Orjuela-Cañon A D, Jutinico A L, Mendoza-Montoya O and Antelis J M 2022 Decoding EEG rhythms offline and online during motor imagery for standing and sitting based on a brain-computer interface *Front. Neuroinform.* **16** 961089
[40] Bugakova A, Nikolaeva V, Gorin A, Muraveva A, Kuzmina E and Lebedev M 2022 EEG during motor imagery under different postural conditions—case study *2022 6th Scientific School Dynamics of Complex Networks and their Applications (DCNA)* 55–7
[41] De Vos M, Gandras K and Debener S 2014 Towards a truly mobile auditory brain-computer interface: exploring the P300 to take away *Int. J. Psychophysiol.* **91** 46–53
[42] Mclaughlin M et al Sedentary Behaviour Council Global Monitoring Initiative Working Group 2020 Worldwide surveillance of self-reported sitting time: a scoping review *Int. J. Behav. Nutr. Phys. Act.* **17** 111
[43] Katzmarzyk P T, Church T S, Craig C L and Bouchard C 2009 Sitting time and mortality from all causes, cardiovascular disease, and cancer *Med. Sci. Sports Exerc.* **41** 998–1005
[44] Patel A V, Bernstein L, Deka A, Feigelson H S, Campbell P T, Gapstur S M, Colditz G A and Thun M J 2010 Leisure time spent sitting in relation to total mortality in a prospective cohort of US adults *Am. J. Epidemiol.* **172** 419–29
[45] Mula A 2018 Ergonomics and the standing desk *Work* **60** 171–4
[46] Minges K E, Chao A M, Irwin M L, Owen N, Park C, Whittemore R and Salmon J 2016 Classroom standing desks and sedentary behavior: a systematic review *Pediatrics* **137** e20153087
[47] Chambers A J, Robertson M M and Baker N A 2019 The effect of sit-stand desks on office worker behavioral and health outcomes: a scoping review *Appl. Ergon.* **78** 37–53
[48] Jung J-Y, Cho H-Y and Kang C-K 2020 Brain activity during a working memory task in different postures: an EEG study *Ergonomics* **63** 1359–70
[49] Bhat M, Dehury K, Chandrasekaran B, Palanisamy H P and Arumugam A 2022 Does standing alter reaction times and event related potentials compared to sitting in young adults? a counterbalanced, crossover trial *Theoretical Issues in Ergonomics Science* **23** 663–86
[50] Caldwell J A, Prazinko B and Caldwell J L 2003 Body posture affects electroencephalographic activity and psychomotor vigilance task performance in sleep-deprived subjects *Clin. Neurophysiol.* **114** 23–31

[51] Xiong J, Hsiang E-L, He Z, Zhan T and Wu S-T 2021 Augmented reality and virtual reality displays: emerging technologies and future perspectives *Light: Sci. Appl.* **10** 216
[52] Ali S G *et al* 2023 A systematic review: virtual-reality-based techniques for human exercises and health improvement *Front. Public Health* **11** 1143947
[53] Al-Ansi A M, Jaboob M, Garad A and Al-Ansi A 2023 Analyzing augmented reality (AR) and virtual reality (VR) recent development in education *Soc. Sci. Humanit. Open* **8** 100532
[54] Putze F, Vourvopoulos A, Lécuyer A, Krusienski D, Bermúdez I Badia S, Mullen T and Herff C 2020 Editorial: Brain-computer interfaces and augmented/virtual reality *Front. Hum. Neurosci.* **14** 144
[55] Lotte F, Faller J, Guger C and Renard Y 2013 Combining BCI with virtual reality: towards new applications and improved BCI *Towards Practical Brain Brain-Computer Interfaces* (Springer) 197–220
[56] Ye Y, Liu L, Hu L and Xia S 2022 Neural3Points: Learning to generate physically realistic full-body motion for virtual reality users *Comput. Graph. Forum* **41** 183–94
[57] Friedman D 2015 Brain-computer interfacing and virtual reality *Handbook of Digital Games and Entertainment Technologies* (Springer) 171
[58] Gehrke L, Lopes P, Klug M, Akman S and Gramann K 2022 Neural sources of prediction errors detect unrealistic VR interactions *J. Neural Eng.* **19** 036002
[59] Gehrke L, Akman S, Lopes P, Chen A, Singh A K, Chen H-T, Lin C-T and Gramann K 2019 Detecting Visuo-Haptic Mismatches in Virtual Reality using the Prediction Error Negativity of Event-Related Brain Potentials *Proc. of the 2019 CHI Conf. on Human Factors in Computing Systems CHI '19* (Association for Computing Machinery) 1–11
[60] Ved H and Yildirim C 2021 Detecting mental workload in virtual reality using EEG spectral data: a deep learning approach *2021 IEEE International Conference on Artificial Intelligence and Virtual Reality (AIVR)* 173–8
[61] Tremmel C, Herff C and Krusienski D J 2019 EEG movement artifact suppression in interactive virtual reality *Conf. Proc. IEEE Eng. Med. Biol. Soc.* **2019** 4576–9
[62] Lécuyer A, George L and Marchal M 2013 Toward adaptive VR simulators combining visual, haptic, and brain-computer interfaces *IEEE Comput. Graph. Appl.* **33** 18–23
[63] Chiossi F, Ou C and Mayer S 2023 Exploring physiological correlates of visual complexity adaptation: insights from EDA, ECG, and EEG data for adaptation evaluation in vr adaptive systems *Extended Abstracts of the 2023 CHI Conf. on Human Factors in Computing Systems CHI EA '23* (Association for Computing Machinery) 1–7
[64] Hubbard R, Sipolins A and Zhou L 2017 Enhancing learning through virtual reality and neurofeedback: a first step *Proceedings of the Seventh International Learning Analytics & Knowledge Conference LAK '17* (Association for Computing Machinery) 398–403
[65] Baker C and Fairclough S H 2022 chapter 9 - Adaptive virtual reality *Current Research in Neuroadaptive Technology* ed S H Fairclough and T O Zander (Academic) 159–76
[66] Freeman D, Haselton P, Freeman J, Spanlang B, Kishore S, Albery E, Denne M, Brown P, Slater M and Nickless A 2018 Automated psychological therapy using immersive virtual reality for treatment of fear of heights: a single-blind, parallel-group, randomised controlled trial *Lancet Psychiatry* **5** 625–32
[67] Marín-Morales J, Higuera-Trujillo J L, Greco A, Guixeres J, Llinares C, Scilingo E P, Alcañiz M and Valenza G 2018 Affective computing in virtual reality: emotion recognition from brain and heartbeat dynamics using wearable sensors *Sci Rep.* **8** 13657
[68] Geraets C N W, van der Stouwe E C D, Pot-Kolder R and Veling W 2021 Advances in immersive virtual reality interventions for mental disorders: a new reality? *Curr Opin Psychol* **41** 40–5
[69] Cieślik B, Mazurek J, Rutkowski S, Kiper P, Turolla A and Szczepańska-Gieracha J 2020 Virtual reality in psychiatric disorders: a systematic review of reviews *Complement. Ther. Med.* **52** 102480
[70] Klug M 2022 Real virtual magic–modifying a VR game with a BCI to enhance immersion *Programme and Proc. of the third Neuroadaptive Technology Conf. (NAT) 2022* 27
[71] Tauscher J P, Schottky F W, Grogorick S, Bittner P M, Mustafa M and Magnor M 2019 Immersive EEG: evaluating electroencephalography in virtual reality *2019 IEEE Conf. on Virtual Reality and 3D User Interfaces (VR)* (IEEE) 1794–800
[72] Weber D, Hertweck S, Alwanni H, Fiederer L D J, Wang X, Unruh F, Fischbach M, Latoschik M E and Ball T 2021 A Structured approach to test the signal quality of electroencephalography measurements during use of head-mounted displays for virtual reality applications *Front. Neurosci.* **15** 733673
[73] Mihajlović V, Grundlehner B, Vullers R and Penders J 2014 Wearable, wireless EEG solutions in daily life applications: what are we missing? *IEEE J. Biomed. Health Inform.* **19** 6–21
[74] Sterr A *et al* 2018 Sleep EEG derived from behind-the-ear electrodes (cEEGrid) compared to standard polysomnography: a proof of concept study *Front. Hum. Neurosci.* **12** 452
[75] Zielasko D and Riecke B E 2021 To sit or not to sit in VR: Analyzing influences and (dis)advantages of posture and embodied interaction *Computers* **10** 73
[76] Gevins A and Smith M E 2003 Neurophysiological measures of cognitive workload during human-computer interaction *Theoretical Issues in Ergonomics Science* **4** 113–31
[77] Klimesch W 1999 EEG alpha and theta oscillations reflect cognitive and memory performance: a review and analysis *Brain Res. Brain Res. Rev.* **29** 169–95
[78] Bowman A D, Griffis J C, Visscher K M, Dobbins A C, Gawne T J, DiFrancesco M W and Szaflarski J P 2017 Relationship between alpha rhythm and the default mode network: an EEG-fMRI study *J. Clin. Neurophysiol.* **34** 527–33
[79] Kam J W, Lin J J, Solbakk A K, Endestad T, Larsson P G and Knight R T 2019 Default network and frontoparietal control network theta connectivity supports internal attention *Nat. Hum. Behav.* **3** 1263–70
[80] Cha H S, Han C H and Im C H 2020 Prediction of individual user's dynamic ranges of EEG features from resting-state EEG data for evaluating their suitability for passive brain–computer interface applications *Sensors* **20** 988
[81] HP Development Company 2024 Available at:https://support.hp.com/us-en/product/details/hp-reverb-g2-omnicept-edition/2100000151
[82] Krol L R, Freytag S-C, Fleck M, Gramann K and Zander T O 2016 A task-independent workload classifier for neuroadaptive technology: Preliminary data *IEEE Int. Conf. on Systems, Man, and Cybernetics (SMC)* (IEEE) 003171–74
[83] Diego S and Swartz U C 2024 Available at: https://github.com/sccn/SNAP
[84] Klem G H, Lüders H O, Jasper H H and Elger C 1999 The ten-twenty electrode system of the International Federation. The international federation of clinical neurophysiology *Electroencephalogr. Clin. Neurophysiol. Suppl.* **52** 3–6
[85] Kothe C *et al* 2024 *bioRxiv* 10.1101/2024.02.13.580071 Posted online: 14 February 2024, Accessed: 24 February 2025
[86] Golding J F 2006 Motion sickness susceptibility *Auton. Neurosci.* **129** 67–76
[87] Kim H K, Park J, Choi Y and Choe M 2018 Virtual reality sickness questionnaire (VRSQ): motion sickness measurement index in a virtual reality environment *Appl. Ergon.* **69** 66–73
[88] Palmer J A, Kreutz-Delgado K and Makeig S 2012 AMICA: An adaptive mixture of independent component analyzers with shared components *Swartz Center for Computational Neuroscience, University of California San Diego Tech. Rep.* 1–15

[89] Klug M, Berg T and Gramann K 2022 No need for extensive artifact rejection for ICA - a multi-study evaluation on stationary and mobile EEG datasets *Bio. Rxiv* **2022** 507772
[90] Delorme A and Makeig S 2004 EEGLAB: an open source toolbox for analysis of single-trial EEG dynamics including independent component analysis *J. Neurosci. Methods* **134** 9–21
[91] Kothe C A and Makeig S 2013 BCILAB: a platform for brain-computer interface development *J. Neural Eng.* **10** 056014
[92] Racine J S 2012 Rstudio: a platform-independent ide for r and sweave *J. Appl. Econometrics* **27** 167–72
[93] Pion-Tonachini L, Kreutz-Delgado K and Makeig S 2019 ICLabel: An automated electroencephalographic independent component classifier, dataset, and website *Neuroimage* **198** 181–97
[94] Welch P 1967 The use of fast fourier transform for the estimation of power spectra: a method based on time averaging over short, modified periodograms *IEEE Trans. Audio Electroacoust.* **15** 70–3
[95] Ang K K, Chin Z Y, Zhang H and Guan C 2008 Filter bank common spatial pattern (FBCSP) in brain-computer interface *2008 IEEE international joint conference on neural networks (IEEE world congress on computational intelligence)* (IEEE) 2390–7
[96] Schuirmann D L 1981 On hypothesis-testing to determine if the mean of a normal distribution is contained in a known interval *Biometrics* **37** 617–617
[97] Imuetinyan D, Willoughby S, Ayodele B and Aghazadeh F 2022 Comparison of muscle activity for sitting and standing positions on a computer workstation *Proc. of the XXXIVth Annual Int. Occupational Ergonomics and Safety Conf. (Int. Society for Occupational Ergonomics and Safety)* 72–5
[98] Altenburg T M, Rotteveel J, Serné E H and Chinapaw M J M 2019 Standing is not enough: a randomized crossover study on the acute cardiometabolic effects of variations in sitting in healthy young men *J. Sci. Med. Sport* **22** 790–6
[99] Heo D, Kim M, Kim J, Choi Y J and Kim S-P 2022 The Uses of Brain-Computer Interface in Different Postures to Application in Real Life *2022 10th Int. Winter Conf. on Brain-Computer Interface (BCI)* 1–5
[100] Zhang K, Xu G, Zheng X, Li H, Zhang S, Yu Y and Liang R 2020 Application of transfer learning in EEG decoding based on brain-computer interfaces: a review *Sensors* **20** 6321
[101] Zhou Y, Xu Z, Niu Y, Wang P, Wen X, Wu X and Zhang D 2022 Cross-task cognitive workload recognition based on EEG and domain adaptation *IEEE Trans. Neural Syst. Rehabil. Eng.* **30** 50–60
[102] Seeber M, Scherer R, Wagner J, Solis-Escalante T and Müller-Putz G R 2014 EEG beta suppression and low gamma modulation are different elements of human upright walking *Front. Hum. Neurosci.* **8** 485
[103] Wagner J, Solis-Escalante T, Scherer R, Neuper C and Müller-Putz G 2014 It's how you get there: walking down a virtual alley activates premotor and parietal areas *Front. Hum. Neurosci.* **8** 93
[104] Debener S, Minow F, Emkes R, Gandras K and de Vos M 2012 How about taking a low-cost, small, and wireless EEG for a walk? *Psychophysiology* **49** 1617–21
[105] Shad E H T, Molinas M and Ytterdal T 2020 Impedance and noise of passive and active dry EEG electrodes: a review *IEEE Sens. J.* **20** 14565–77
[106] Di Flumeri G, Aricò P, Borghini G, Sciaraffa N, Di Florio A and Babiloni F 2019 The dry revolution: evaluation of three different EEG dry electrode types in terms of signal spectral features, mental states classification and usability *Sensors* **19** 1365
[107] Marini F, Lee C, Wagner J, Makeig S and Gola M 2019 A comparative evaluation of signal quality between a research-grade and a wireless dry-electrode mobile EEG system *J. Neural Eng.* **16** 054001
[108] Zander T O, Lehne M, Ihme K, Jatzev S, Correia J, Kothe C, Picht B and Nijboer F 2011 A dry EEG-system for scientific research and brain–computer interfaces *Front. Neurosci.* **5** 53
[109] Li G-L, Wu J-T, Xia Y-H, He Q-G and Jin H-G 2020 Review of semi-dry electrodes for EEG recording *J. Neural Eng.* **17** 051004
[110] Klug M and Gramann K 2021 Identifying key factors for improving ICA-based decomposition of EEG data in mobile and stationary experiments *Eur. J. Neurosci.* **54** 8406–20
[111] Debener S, Emkes R, De Vos M and Bleichner M 2015 Unobtrusive ambulatory EEG using a smartphone and flexible printed electrodes around the ear *Sci. Rep.* **5** 16743
[112] Pion-Tonachini L, Hsu S-H, Makeig S, Jung T-P and Cauwenberghs G 2015 Real-time EEG Source-mapping Toolbox (REST): online ICA and source localization *Conf. Proc. IEEE Eng. Med. Biol. Soc.* **2015** 4114–7